The Cryosphere

Gas diffusivity and permeability through the firn column at Summit, Greenland: measurements and comparison to microstructural properties

A. C. Adolph and M. R. Albert

Thayer School of Engineering, Dartmouth College, Hanover, NH, USA

Correspondence to: M. R. Albert (mary.r.albert@dartmouth.edu)

Abstract. The physical structure of polar firn plays a key role in the mechanisms by which glaciers and ice sheets preserve a natural archive of past atmospheric composition. This study presents the first measurements of gas diffusivity and permeability along with microstructural information measured from the near-surface firn through the firn column to pore close-off. Both fine- and coarse-grained firn from Summit, Greenland are included in this study to investigate the variability in firn caused by seasonal and storm-event layering. Our measurements reveal that the porosity of firn (derived from density) is insufficient to describe the full profiles of diffusivity and permeability, particularly at porosity values above 0.5. Thus, even a model that could perfectly predict the density profile would be insufficient for application to issues involving gas transport. The measured diffusivity profile presented here is compared to two diffusivity profiles modeled from firn air measurements from Summit. Because of differences in scale and in firn processes between the true field situation, firn modeling, and laboratory measurements, the results follow a similar overall pattern but do not align; our results constitute a lower bound on diffusive transport. In comparing our measurements of both diffusivity and permeability to previous parameterizations from numerical 3-D lattice-Boltzmann modeling, it is evident that the previous relationships to porosity are likely site-specific. We present parameterizations relating diffusivity and permeability to porosity as a possible tool, though use of direct measurements would be far more accurate when feasible. The relationships between gas transport properties and microstructural properties are characterized and compared to existing relationships for general porous media, specifically the Katz–

Thompson (KT), Kozeny–Carman (KC), and Archie's law approximations. While those approximations can capture the general trend of gas transport relationships, they result in high errors for individual samples and fail to fully describe firn variability, particularly the differences between coarse- and fine-grained firn. We present a direct power law relationship between permeability and gas diffusivity based on our co-located measurements; further research will indicate if this type of relationship is site-specific. This set of measurements and relationships contributes a unique starting point for future investigations in developing more physically based models of firn gas transport.

1 Introduction

Firn is a complex porous material, comprised of aged snow more than one year old. It separates the atmosphere from the underlying solid glacial ice which archives a unique record of atmospheric history. In dry-snow zones, the firn comprises approximately 60 to 120 m of depth in the top of the polar ice sheets. While firn initiates as snow on the surface, the pore space of the firn becomes increasingly compacted with depth due to overburden pressure, metamorphism, and sintering. With this increasing compaction, the interconnected pore space ultimately becomes transformed into individual bubbles of air. Samples of the ancient atmosphere stored in these bubbles can provide insight into past climate (e.g., Neftel et al., 1982; Raynaud et al., 1993; Blunier and Brook, 2001). Because the air diffuses through the open pore space more rapidly than the snow turns to bubbly ice, the age of

the ice and the age of the air inside the bubbles at a given depth is not the same (Schwander et al., 1993). Furthermore, this age difference is actually represented by a distribution and not a discrete number because of the smoothing effects of diffusive gas transport near pore close-off (Spahni et al., 2003). These attenuation effects as well as the age difference between ice and air have important implications for interpreting ice core records, particularly with respect to leads and lags between climate proxy information in the ice and atmospheric gas records in the bubbles. However, there remain many uncertainties in constraining the effects of these processes because of the complexities of firn air transport (Brook, 2013; Trudinger et al., 2013).

An important factor in understanding the firn record of past atmospheric composition is an understanding of the impact of the layered physical structure of firn on gas movement through the firn column. Two of the physical properties of interest are effective gas diffusivity and permeability. Several studies have investigated these important gas transport metrics of firn in the past. Albert and Shultz (2002) conducted field measurements of SF_6 diffusivity in the surface windpack layer at Summit using an in situ technique developed for air–snow transfer applications. Schwander et al. (1988) and Fabre et al. (2000) made laboratory measurements of firn diffusivity using an elution peak technique. Adolph and Albert (2013) designed and verified a different technique for direct measurements of the gas diffusivity of firn; this technique is based on the measurement of purely diffusive transport, instead of extrapolation from convective transport measurements. Laboratory measurements of permeability have been made in firn, though none down through pore close-off (e.g., Albert et al., 2000; Rick and Albert, 2004; Courville et al., 2007; Hörhold et al., 2009). Additionally, lattice-Boltzmann modeling informed by 3-D microstructural reconstructions of firn have been used to investigate gas diffusivity and permeability in firn (Freitag et al., 2002; Courville et al., 2010).

This study presents the first collection of co-located gas diffusivity, permeability, and microstructural measurements made on the same samples from the firn column from near surface through pore close-off. The results are compared to the work that has been done to characterize the physical properties of firn, described above. This unique set of measurements also allows for a comparison to studies of the nature of gas transport through general porous materials. The Katz–Thompson approximation, Kozeny–Carman approximation, and Archie's law are all used to investigate how firn compares to idealized porous media. Understanding these relationships can lay the foundation for parameterizing gas transport properties in a way that could improve firn gas transport modeling. Additionally, understanding the relationships between gas transport and microstructure may illuminate instances where generalized parameterizations might fall short.

2 Methods

2.1 Firn samples and site location

This study focuses on firn from the top 85 m of the ice sheet at Summit, Greenland. In the 2007 field season a firn core was extracted, and it has remained in storage at $-29\,^{\circ}C$ at the Cold Regions Research and Engineering Laboratory in Hanover, NH. Density and permeability measurements were made on the full firn core shortly after collection, and then again on select samples used in this study in 2012. On average, the difference in density between the two measurements was -1.5%, which is within the error of the density measurements. The maximum density differences occurred on fragile pieces that had become damaged with repeated handling. Aside from the complete profiles of permeability and density (Figs. 1 and 2), all measurements in this study were made within a several month time span, and permeability and density on the selected samples were remeasured in this same window. Due to the short time frame of laboratory measurements, and the fact that measurable differences did not occur over the multiyear-long storage, the results are consistent and can reliably be compared to one another without considering the effects of metamorphism occurring during storage. The relationships developed between parameters considered in this study are derived from measurements which are co-located both physically and temporally.

The firn core is approximately 8 cm in diameter, and it has been cut into lengths ranging from 2 to 12 cm, based on stratigraphy. Visual inspection of firn core samples on a backlit table enabled characterization of layering in the core on a gradual scale from coarse-grained to fine-grained. Some samples are single layers which are homogeneous in their grain size, while others contain multiple layers of firn. The firn air campaign completed at Summit during the year that this core was collected found that the lock-in zone started at 69 m depth, and the lock-in depth occurred at 80 m (Faïn et al., 2009), so the samples in the present study represent the full firn column from near surface down through the pore close-off depth.

2.2 Porosity

The density of each firn sample was determined using a digital balance (instrument error: ± 0.01 g) and dial calipers (instrument error: ± 0.001 cm) for mass and volume determination. Total porosity is then calculated as $\phi = 1 - \rho(z)/\rho_{\text{ice}}$, where $\rho(z)$ is the density of the firn sample at a depth z, and p_{ice} is the density of pure ice. Any nonuniformity in the geometry of the sample can lead to errors in density (and subsequent porosity) measurement. These geometric discrepancies, if present, are typically one millimeter or less. In the case of the smallest possible sample (2 cm in height and 8 cm in diameter), with a maximum variability in geometry (± 0.1 cm for height, ± 0.05 cm for diameter), the volumetric

calculation could be off by up to 6.3 %. This would represent the most extreme error and is not representative of typical error.

In the study of gas transport, it is often only the open porosity that is relevant to processes under investigation. Open porosity is not trivial to measure directly, so parameterizations such as those developed by Schwander (1989) or Goujon et al. (2003) are often used to approximate the open porosity, which can be calculated as $\phi_o = \phi - \phi_c$, where ϕ_c is the closed porosity. We approximated closed porosity using the Schwander (1989) empirical relationship as follows:

$$
\phi_c = \begin{cases} \phi \exp\left[75 * \left(\frac{\rho(z)}{\rho_{co}} - 1\right)\right], & 0 < \rho(z) < \rho_{co}, \\ \phi & , \rho(z) \geq \rho_{co} \end{cases} \tag{1}
$$

where $\rho(z)$ is the density of the firn sample, and ρ_{co} is the density of the firn at pore close-off depth. Recent work has shown that close-off depth typically does not actually occur at a single density, but over a range of densities depending on firn grain sizes (Gregory et al., 2014). However, for the purpose of the Schwander parameterization, the close-off density is estimated from the Martinerie et al. (1994) parameterization, which yields a value of $0.823\,\mathrm{g\,cm^{-3}}$ at Summit conditions.

This approximation only significantly affects the samples whose total porosity is less than 0.2. When considering the subset of samples that were used for diffusivity measurements, only 5 of the 46 selected samples have a significant closed porosity. For analyses which only include these samples, the Schwander approximation will not be used. We will instead present our results in terms of total porosity, with the knowledge that using open porosity instead would not significantly change the outcomes of our analyses but would add unnecessary assumptions about pore close-off mechanics. In cases where all samples from the entire firn core are considered, the Schwander approximation will be implemented, as a significant number of samples have measurable closed porosity. Throughout the text, a distinction will be made to note when the Schwander approximation for open porosity is used and what effect it has on the analysis.

2.3 Gas diffusivity measurement

Gas diffusivity is a gas transport metric related to Fick's laws of diffusion describing the transport of particles as a result of concentration gradients. Gas diffusivity was measured on selected firn samples using a technique design for use on firn cores that has been validated on glass beads (Adolph and Albert, 2013). SF_6 was used as the diffusing gas in the measurements because it is inert, and thus the results will only be affected by the geometrical properties of the firn, and not by any chemical interactions or sorption. For the measurements, the firn sample is placed in a sealed holder which is attached to a closed chamber on each side. SF_6 is injected into the initial chamber and then allowed to diffuse through the sample

and into the exit chamber over time. Concentration is monitored in the initial chamber, and the profile of concentration over time is used to determine the diffusivity using a numerical solution for Fick's second law of diffusion:

$$
\frac{\partial c}{\partial t} = D_f \frac{\partial^2 c}{\partial z^2}, \tag{2}
$$

where c is the gas concentration, t represents time, D_f is the diffusivity of the firn sample, and z is the position in the firn. The SF_6 concentrations are measured using a Lagus Applied Technology Autotrac 101 gas chromatograph. Diffusivity measurements were made on 46 firn core samples from depths in the ice sheet that ranged between 1.7 and 70.7 m. Samples were determined to be homogeneous by inspection on a backlit table, and grain size in the layers were characterized on a scale from fine- to coarse-grained. Based on seven repeated experiments on one glass bead sample, the standard deviation of the measurements was 13 %. Possible sources of error include incomplete mixing in end chambers, errors of the gas chromatograph (± 0.3 % of the measured concentration, as stated by manufacturer), or errors in the timing of sample extraction (less than 5 s).

2.4 Permeability measurement

Permeability is defined in Darcy's law as the factor relating air flow velocity resulting from a pressure differential across a porous medium as follows:

$$
v = \frac{k}{\mu} \frac{dP}{dz}, \tag{3}
$$

where k is permeability, v is the air flow velocity, μ is the dynamic viscosity, and P is the pressure. Permeability was measured on each firn sample from the entire firn core, from the surface down to 90 m depth. It is measured along the vertical axis of the core samples, which ranged in height from 2 to 12 cm. To determine permeability, the firn sample is subjected to a variety of different flow velocities, and at each distinct flow velocity the pressure differential across the sample is measured. For flows in the linear range, the permeability is calculated from Darcy's law using the measured air flow rate, pressure drop, temperature, and barometric pressure (Albert et al., 2000). For each sample, 5–10 measurements are made at different flow velocities, and mean values are reported. Differences in these replicate measurements on the same sample are less than 5 % in firn above 50 m and less than 10 % in firn below 50 m. Based on 10 repeated measurements on different samples of firn from the same layer in the field, the error of the measurement as an indicator of layer permeability is less than 10 %. The lowest measurable permeability is $0.01 \times 10^{-10}\,\mathrm{m^2}$; therefore in this study, any sample with permeability below that value is considered impermeable.

2.5 Microstructural properties

Of the select firn samples, 18 fine-grained samples and 11 coarse-grained samples were imaged using a Skyscan 1172 microCT scanner in a temperature-controlled room held at $-12\,°C$. A microfocus X-ray tube provides a fixed source ($40\,kV$ and $250\,µA$) as the firn sample is rotated in $0.7°$ steps to complete $180°$ of rotation. This creates a series of shadowed vertical images with a pixel size of $14.8\,µm$ which are then compiled using NReconn software to generate a stack of horizontal images in greyscale. Because the ice phase and the air phase of the firn structure have such different attenuation coefficients, a constant threshold separating the ice phase from the air phase was used to divide the 256 bits of greyscale: 0–89 for the ice phase and 90–256 for the air phase. Artifacts smaller than 25 voxels (a 3-dimensional pixel) are removed using the CTAn software. The samples used for imaging were $1\,cm \times 1\,cm \times 1.5\,cm$ in size, and to reduce edge effects, only the inner $0.7\,cm \times 0.7\,cm \times 1\,cm$ are used in the analysis. The microCT provides a 3-D image of the firn and the pores, and a number of physical parameters are calculated from the image data which describe the microstructure of the firn. The parameters of interest are the specific surface area (SSA) and the average circular equivalent diameter (d_{eq}). The SSA is a ratio of the surface area of the pores (S) to the total volume of the firn sample (V_p); this can indicate the complexity of the firn (Lomonaco et al., 2011). d_{eq} is calculated on 2-D slices as the diameter of a circle that has the equivalent area to a given pore. The average for each of the samples imaged is taken for all of the pores in that sample. Though this parameter is not traditionally used in gas transport applications, it provides an unbiased characteristic size of the pore space.

3 Results and discussion

3.1 Gas diffusivity and permeability profiles

Figure 1 shows the profiles of permeability and normalized gas diffusivity as a function of density. For reference, the density profile made on the same pieces of the firn is shown in Fig. 2. The measured permeability on samples between the surface and $85\,m$ depth ranged from impermeable in the deepest parts of the firn to $177 \times 10^{-10}\,m^2$ several meters below the snow–air interface. The general shape of the permeability profile is the same as measured in the top ten meters on a different shallow core from Summit in an earlier study (Albert and Shultz, 2002). The maximum permeability occurs below the firn surface due to the post-depositional metamorphism on aged firn and the lower permeability of the more recent windpack surface layers (Albert and Shultz, 2002). Gas diffusivity results were normalized by dividing the measured gas diffusivity of the firn sample (D_f) by the free-air diffusivity of SF_6 at experimental temper-
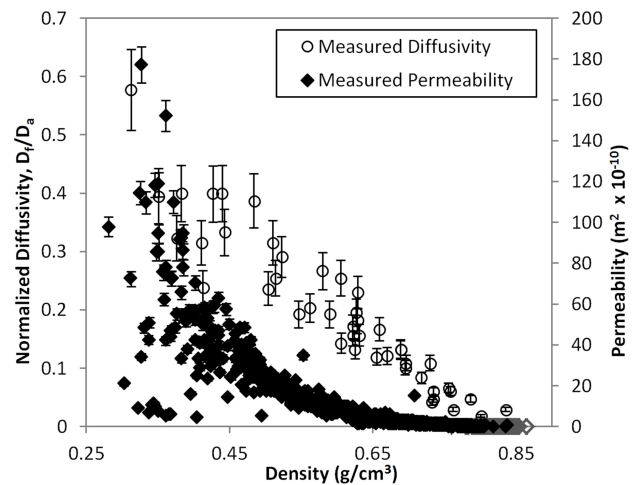

Fig. 1. Normalized diffusivity and permeability vs. density for discrete firn samples from Summit, Greenland. Grey diamonds indicate samples which were determined to be impermeable. Diffusivity error bars show 13 % error, estimated from repeat measurements on a single sample. Permeability error bars show approximately 5 % error above 50 m and 10 % error below 50 m.

ature and pressure conditions ($T = 260\,K$, $P = 1000\,mbar$, $D_a = 0.0836\,cm^2\,s^{-1}$) (Matsunaga et al., 2002). The normalized results ranged from 0.02 in the deep lock-in zone of the firn to 0.58 in near-surface firn. Using a different in situ measurement device, Albert and Shultz (2002) determined the normalized diffusivities of near-surface windpacked snow to be 0.57 and 0.64, which are comparable to our near-surface firn measurements.

As seen in Fig. 1, density is not a clear indicator of either diffusivity or permeability, as a given density could correspond to a range of values for diffusivity or permeability. Each obeys a general trend with depth caused by increasingly limited pore space due to firn compaction. Density generally increases with depth while permeability and diffusivity decrease; however, layering in firn and post-depositional metamorphism cause measurable variations from these general trends. The variability of density caused by layering and heterogeneity in the firn cannot fully describe the variability in the permeability and diffusivity measurements. Density is defined as mass per unit volume, but it does not provide any information about the arrangement of the mass within that volume, which is critical to rates of interstitial gas transport. Overall, the diffusivity profile does not exhibit the same shape as the permeability profile, indicating that these two parameters do not have a constant linear relationship, and that these two gas transport metrics are dependent, to some extent, on different microstructural properties. While firn permeability measurements on a single sample take on the order of 10 min, gas diffusivity measurements take on the order of 3–5 h per sample. Developing a reliable, accurate relationship between the two properties could help us to extrapolate
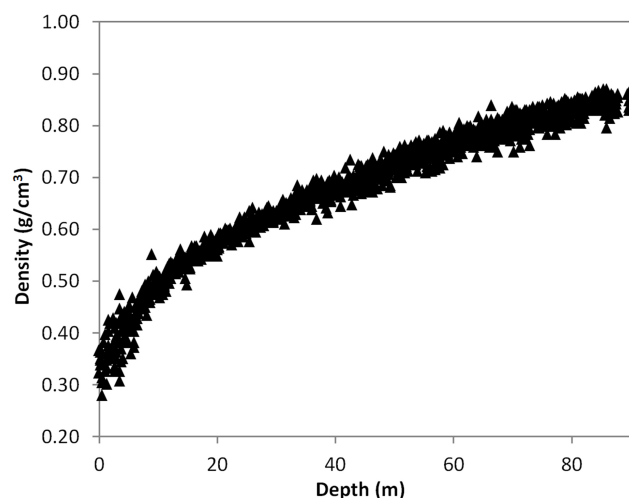
Fig. 2. Density profile for the firn at Summit, Greenland.

Fig. 3. Comparison of measured diffusivity to diffusivity modeled from firn air measurements at Summit, Greenland. Error bars show 13 % error, estimated from repeat measurements on a single sample.

our permeability measurements on firn cores from other sites to provide information about diffusion processes at these sites. We will revisit the development of such a relationship after determining how these measurements compare to previous published literature on gas transport in firn.

3.2 Comparison to modeled diffusivity from firn air campaigns

Our direct diffusivity measurements are compared to two CO_2 diffusivity profiles that were determined by firn air modeling from Summit, Greenland, developed by C. Buizert (personal communication, 2013) and M. Battle (personal communication, 2012). To facilitate this comparison, our laboratory measurements of diffusivity are normalized by dividing by the free-air diffusivity of SF_6 at experimental temperature and pressure conditions, and the CO_2 diffusivity profiles are normalized by the free-air diffusivity of CO_2 at Summit temperature and pressure conditions. With $T = -31.4\,^\circ C$ and $P = 665\,hPa$ (Schwander et al., 1993; Witrant et al., 2012), the free-air gas diffusivity of CO_2 at Summit is $D_{CO_2,air} = 0.18\,cm^2\,s^{-1}$ (Matsunaga et al., 1998). In Fig. 3 we show the comparison of measured and modeled diffusivity as the ratio of diffusivity in firn (D_f) to the diffusivity in free air (D_a). Our results confirm what was shown to be true for firn studies in Antarctica and France by Fabre et al. (2000); modeled parameterizations of diffusivity result in much higher values than what is measured on discrete firn samples in the laboratory. Due to the difference in scale, the laboratory measurements are reflecting effective molecular diffusivity through firn due to firn structure, while parameterizations in firn air models also incorporate the possibility of larger-scale transport processes and spatial heterogeneity in firn structure (Buizert et al., 2012; Fabre et al., 2000). However, it is of note that there are regions of the firn column where the models disagree with one another
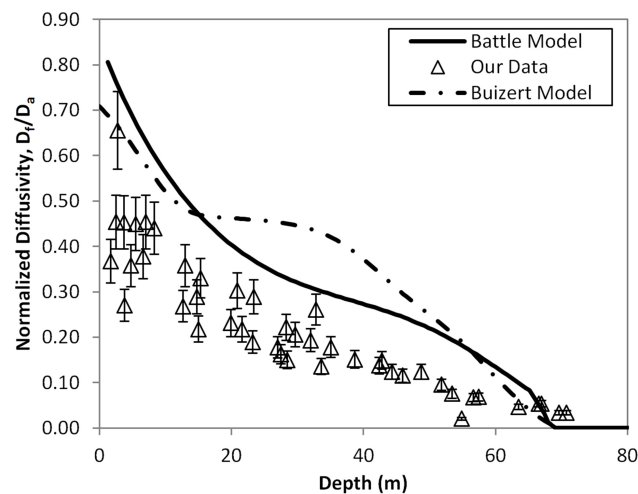
to the same degree that our laboratory measurements disagree with the models. The laboratory measurements of the effective inert gas molecular diffusivity serve as a definitive lower bound for the rate of diffusion, and the discrepancies between the molecular diffusivities and the modeled parameterizations warrant future investigations. The effective inert gas molecular diffusivities are a useful tool in characterizing the physical mechanics of gas transport, particularly when microscale physics are concerned. Future investigations will examine larger-scale phenomena that represent different aspects of gas transport in deep firn.

3.3 Comparison to 3-D microscale modeling of permeability and diffusivity

Numerical investigations of gas diffusivity and permeability based on lattice-Boltzmann modeling have been published; Freitag et al. (2002) used three-dimensional reconstructions of firn from the North Greenland Traverse (approximately 450 km northwest of Summit) as inputs for modeling to calculate gas diffusivity and permeability. The reconstructions were developed from samples that were approximately $3\,cm \times 4\,cm \times 4\,cm$ and ranged in porosity from approximately 0.04 to 0.5. Three-dimensional models were created by using a microtome to remove one layer at a time and imaging between each cut. Their modeling results showed that permeability was related to open porosity (ϕ_o) by a power law with exponent 3.4, and diffusivity was related to open porosity by a power law with exponent 2.1 as follows:

$$k = 10^{-7.7}\,m^2\phi_o^{3.4} \qquad \frac{D_f}{D_a} = \phi_o^{2.1}. \qquad (4)$$

A comparison between these results and our measurements can be seen in Fig. 4. To provide consistency with the Freitag
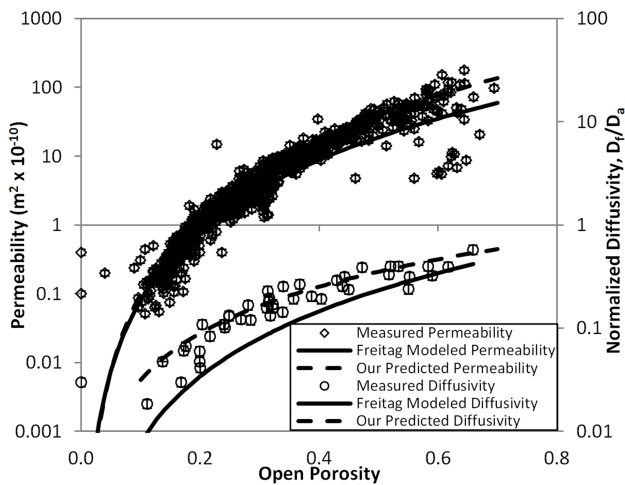
Fig. 4. Logarithmic scale of measured permeability and normalized diffusivity plotted against porosity, showing the permeability and diffusivity formulas developed by Freitag et al. (2002) using lattice-Boltzmann modeling, and our parameterizations based solely on measurements: for permeability, $k = 10^{-7.29} \, \mathrm{m}^2 \phi_\mathrm{o}^{3.71}$ and $R^2 = 0.66$, and for diffusivity, $D_\mathrm{f} / D_\mathrm{a} = \phi^\mathrm{m}$ with $m = 1.5$. $R^2 = 0.852$.

results, we use the Schwander (1989) closed porosity parameterization here to plot our measurements vs. open porosity as opposed to our measured total porosity. This only changes the results for samples that have a total porosity below 0.2. If the comparison were left with our measured results plotted against total porosity instead of open porosity, the Freitag relationship would obviously over predict the permeability for a given porosity because not all of the total porosity is available for transport. However, there is significant natural variability in the permeability and diffusivity measurements values such that the effects of plotting the data vs. open or total porosity is difficult to notice. Considering differences in site location and sample size, the permeability results follow similar trends for low open porosities, but at high porosities the Freitag et al. (2002) relationship underestimates measured permeability. The gas diffusivity results are consistently underestimated by the Freitag relationship. Predictions of permeability and diffusivity based on the lattice-Boltzmann modeling from microstructure are not generally applicable relationships. This may be due to difference in sample size or site differences that cannot be fully explained by open porosity.

3.4 Parameterizations of measured diffusivity and permeability based on open porosity

Our measured values of diffusivity and permeability allow us to create parameterizations based on porosity. Because the full permeability profile includes samples of the entire firn column and contains many samples with a significant closed porosity, the Schwander parameterization (Eq. 1) is used to

estimate open porosity from our measured total porosity in this case. Using the same power law form employed in Freitag et al. (2002), a permeability parameterization based on a least squares method was found:

$$k = 10^{-7.29} \mathrm{m}^2 \phi_\mathrm{o}^{3.71}. \tag{5}$$

A comparison between this parameterization and the data can be seen in Fig. 4. While the parameterization has an R^2 value of 0.66, it is clear that there is a significant amount of scatter in the data at high porosities, which reveals that open porosity is a poor indicator of permeability in that range. If our measured total porosity were used directly to generate a similar parameterization, the best-fit equation would be $k = 10^{-7.53} \mathrm{m}^2 \phi^{2.74}$, but the fit is poor ($R^2$ value of 0.51). In particular, it overpredicts permeability for most of the range of porosities considered in order to artificially fit points at low porosity. It also suffers the same flaw as any parameterization based solely on porosity; there is much more natural variability in firn structure than the porosity alone can describe. There is significant focus in the firn community on density and densification processes, which in turn yields porosity values, but our direct measurements show that, even if density is expressly known, it cannot capture the variability in permeability. In near-surface firn where convection takes place, permeability is a critical component of determining rates of gas transport. However, this is where parameterizations based on porosity are least effective because of the large spread in permeability for a given porosity. Implementing direct measurements of permeability (along with pressure gradients) in physically based models of gas transport should improve the representation of convection in an area where the parameterizations are not as reliable (e.g., as suggested in Witrant et al., 2013).

The Freitag et al. (2002) relationship for normalized diffusivity is a form of Archie's law, which is often cited in porous media literature to relate porosity to both fluid transport and electrical conductivity (Garboczi, 1990). The general form is ϕ^m, where m is experimentally determined for each material and is typically a value between 1 and 2. From our diffusivity results, the average m value for Summit firn is 1.50. Figure 4 shows this Archie's law approximation with our measured results. This approximation fits the data with an R^2 value of 0.852.

3.5 Comparison to idealized porous media

In the study of generalized porous media, previous relationships including other microstructural properties beyond porosity have been developed to relate diffusivity and permeability. Two particularly well-known relationships are the KC and the KT theories. The Kozeny–Carman approximation is derived by assuming a collection of cylindrical tubes, and solving for the flow through them. The solution is generalized by multiplying by a coefficient to be determined experimentally. It has proven particularly useful in the study
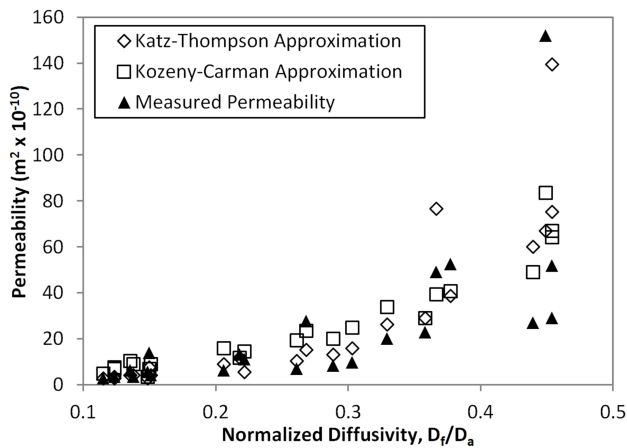
Fig. 5. Measured permeability of Summit, Greenland firn samples compared to Kozeny–Carman and Katz–Thompson approximations.

of powders (Garboczi, 1990; Schwartz et al., 1993). The formula is as follows:

$$k = \frac{\left(\frac{V_p}{S}\right)^2}{2F} \approx \frac{1}{2}\left(\frac{1}{\mathrm{SSA}}\right)^2\left(\frac{D_f}{D_a}\right), \qquad (6)$$

where F is the formation factor, which is equal to the inverse of the normalized diffusivity, D_f/D_a (Schwartz et al., 1993). The Katz–Thompson approximation is developed from percolation theory and requires a critical pore diameter and a measure of the sample conductivity of the pore space, which is then linked to the formation factor (Garboczi, 1990). The Katz–Thompson approximation is as follows:

$$k = \frac{cd_c}{F} \approx cd_{eq}\frac{D_f}{D_a}, \qquad (7)$$

where d_c is the critical pore diameter and c is a calculated (not experimentally determined) constant with a value of $1/226$ (Katz and Thompson, 1986). The critical pore diameter is a measurement of the narrowest part of the set of pores that are connected through the whole sample; the maximum diameter at that point is the critical pore diameter. Critical pore diameter is typically determined by mercury intrusion experiments (Garboczi, 1990); in this study, due to the lack of a parameter equivalent to the critical pore diameter, we approximate it using an average equivalent circle pore diameter determined through microCT scanning. Using this approximation, the Katz–Thompson theory provides an upper bound on permeability because the critical pore diameter is smaller than the average pore diameter. Figure 5 shows the measured permeability as compared to these two different approximations.

Though the general shape of the measured permeability curve is reflected in the approximations, there are large deviations (up to an order or magnitude) between the two across

Table 1. Summary statistics of the percentage errors of the Katz–Thompson and Kozeny–Carman approximations.

	Fine-grained firn		Coarse-grained firn	
	Mean	Standard deviation	Mean	Standard deviation
Katz–Thompson approximation percent error	44.95	61.48	−10.91	53.27
Kozeny–Carman approximation percent error	126.37	82.84	57.49	152.60

the whole range of porosities investigated. These deviations are evident in the plot of percent error between measured and approximated permeability, shown in Fig. 6. It is of note that the errors of the approximations differ for the coarse- and fine-grained firn samples. In both the KT and KC approximations, permeability is more frequently underestimated for coarse-grained samples and overestimated for fine-grained samples (see Fig. 6). There is very clearly one sample whose permeability is grossly overestimated by the KT and KC theories. This sample has nearly the lowest measurable permeability, and it is clear that the approximations are not able to capture this. The error of the Archie's law approximation does not show this same trend; the sign of the error is independent of the grain size. The means and standard deviations of the KC and KT approximation errors are shown in Table 1, with the lowest measurable permeability sample excluded from the set.

The relationships derived from idealized porous media should not be directly applied to firn, as there are clear differences between the measurements and the approximated values. This indicates that firn structure has complexities which cannot be described through idealized porous media.

3.6 Microstructural characteristics of firn as relevant to gas transport

To determine the cause of the difference in coarse- and fine-grained particles as seen in the KT and KC approximations, we turn to the microstructural properties under investigation. Figure 7 shows specific surface area and d_{eq} as a function of total porosity. Both of the parameters used in the KT and KC approximations show different trends for coarse and fine particles. For d_{eq}, fine-grained firn shows a steeper slope as a function of porosity than does the coarse-grained firn. The opposite is true for specific surface area; the SSA of coarse-grained firn is more sensitive to porosity than fine-grained firn. Differences between fine- and coarse-grained firn are also evident in the relationship between diffusivity and permeability. Figure 8 shows measured permeability as a function of normalized diffusivity. A best-fit parameterization was created to define the relationship between diffusivity
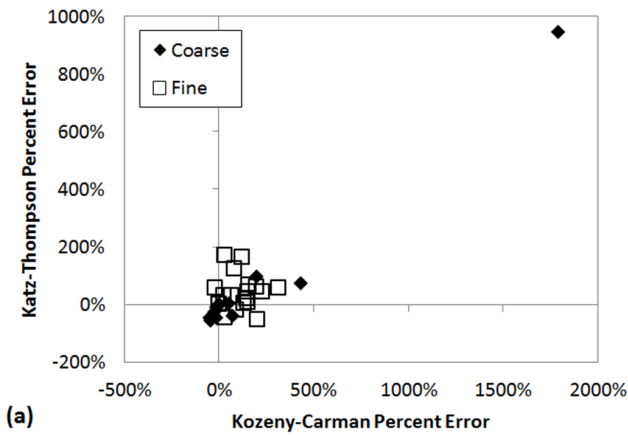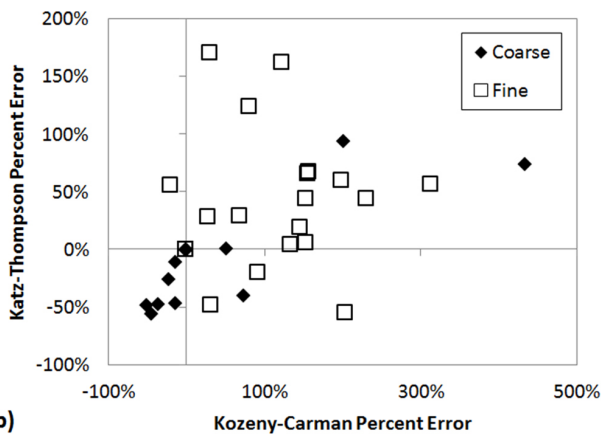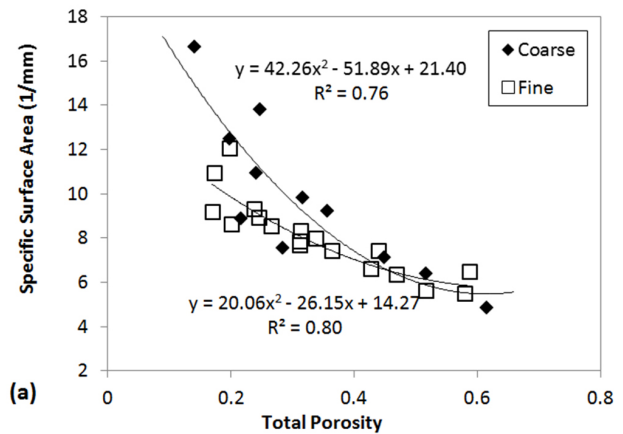
Fig. 6. (a) Percent error between approximated and measured permeability for the Katz–Thompson and Kozeny–Carman approximations. **(b)** Same as **(a)** with the outlier point (as described in text) removed.
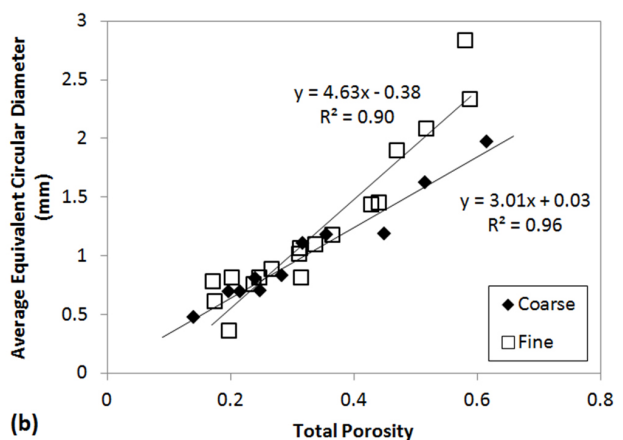

Fig. 7. (a) Specific surface area vs. total porosity; **(b)** Average equivalent circular diameter vs. total porosity.

and permeability and the result is as follows:

$$k = 10^{-6.973}\,\mathrm{m}^2 \left(\frac{D_f}{D_a}\right)^{2.79}. \tag{8}$$

The fit has an R^2 value of 0.745. This figure also reveals that coarse-grained firn tends to have a higher permeability for a given diffusivity than does fine-grained firn. This may explain why the Katz–Thompson and Kozeny–Carman relationships were underpredicting the permeability of coarse-grained firn. It appears that the relationship between diffusivity and permeability is sensitive to the grain size of the firn sample. Lomonaco et al. (2011) conducted an analysis of firn microstructure on fine-grained firn samples from many layers through the firn column; the fine-grained layers studied had originated from winter snow accumulation. In future studies, we will address seasonal differences in permeability, diffusivity, and microstructure and the evolution of layering in the firn column.

4   Conclusions

We have presented the first co-located measurements of diffusivity, permeability, and microstructure on samples throughout the firn column. Our measurements show that density (and porosity derived from density measurements) fails to capture the profile of diffusivity and permeability, particularly in the near-surface firn. Thus, even a model that could perfectly predict a density profile would be insufficient to fully describe interstitial gas transport. The measured gas diffusivity profile presented here places a definitive lower bound for gas transport in firn. Comparisons with two inferred gas diffusivity profiles resulting from modeling of firn air show clear differences that are likely due to spatial variations in physical properties and larger-scale transport phenomena; future work will further investigate these differences.

Comparison of these measurements to Freitag et al. (2002) parameterizations based on lattice-Boltzmann modeling revealed that the equations match our measured permeability values fairly well except at high porosities, where measured permeability values exceed the Freitag parameterization.
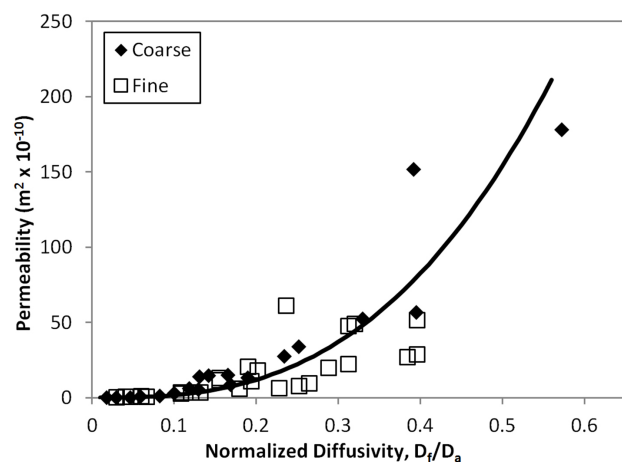
Fig. 8. Measured permeability vs. measured normalized diffusivity. A best-fit relationship between the two parameters is shown as follows: $k = 10^{-6.973}\,\mathrm{m}^2 \left(\frac{D_{\mathrm{f}}}{D_{\mathrm{a}}}\right)^{2.79}$.

Diffusivity is underestimated across the whole range of porosities by the Freitag parameterization. The anomalies between our measured values and these parameterizations are potentially due to differences in firn site characteristics, as the Freitag site is approximately 450 km northwest of Summit. This further indicates that open porosity is not enough to create a general characterization of diffusivity and permeability, as the relationships are likely site-specific. We presented similar best-fit parameterizations based solely on open porosity and our measured diffusivity and permeability profiles to document the relationship from this core for Summit firn; however, these types of relationships will systematically fail to capture the high variability of permeability and diffusivity at high porosities in near-surface firn, particularly at porosity values about 0.5. As a result, representations of gas transport in firn would be well served to use measured permeability or diffusivity instead of parameterizations at porosities above 0.5 when possible. Our unique set of measurements has also allowed us to compare gas transport in firn to other porous media. The Katz–Thompson and Kozeny–Carman approximations show the general trend of the relationship between diffusivity and permeability, but they do not accurately predict individual permeability values. In particular, there are clear differences between fine- and coarse-grained firn which are not captured by the Katz–Thompson and Kozeny–Carman approximations. The relationship between diffusivity and permeability is clearly nonlinear, and a power law relationship derived exclusively from laboratory measurements is presented (Eq. 8). With an R^2 value of 0.745, the variability of the two parameters is captured, and it warrants investigation to determine if such a parameterization would be applicable to other polar sites and which climactic variables might affect this relationship.

Though this firn core was extracted prior to the recent widespread Greenland melt event in 2012 (Nghiem et al., 2012), it is clear that climactic conditions at Summit are changing rapidly, and melt events may become more likely (McGrath et al., 2013). Rapid warming and more frequent ice layers will certainly change the structure of the firn, and the effects of these changes on gas transport properties will be the subject of future investigations.

References

Adolph, A. and Albert, M. R.: An improved technique to measure firn diffusivity, Int. J. Heat Mass Tran., 61, 598–604, 2013.

Albert, M. R. and Shultz, E. F.: Snow and Firn Properties and Air-Snow Transport Processes at Summit, Greenland, Atmos. Environ., 36, 2789–2797, 2002.

Albert, M. R., Shultz, E. F., and Perron, F. E.: Snow and firn permeability at Siple Dome, Antarctica, Ann. Glaciol., 31, 353–356, 2000.

Blunier, T. and Brook, E. J.: Timing of millennial-scale climate change in Antarctica and Greenland during the last glacial period, Science, 291, 109–112, 2001.

Brook, E. J.: Leads and Lags at the End of the Last Ice Age, Science, 339, 1042–1043, 2013.

Buizert, C., Martinerie, P., Petrenko, V. V., Severinghaus, J. P., Trudinger, C. M., Witrant, E., Rosen, J. L., Orsi, A. J., Rubino, M., Etheridge, D. M., Steele, L. P., Hogan, C., Laube, J. C., Sturges, W. T., Levchenko, V. A., Smith, A. M., Levin, I., Conway, T. J., Dlugokencky, E. J., Lang, P. M., Kawamura, K., Jenk, T. M., White, J. W. C., Sowers, T., Schwander, J., and Blunier, T.: Gas transport in firn: multiple-tracer characterisation and model intercomparison for NEEM, Northern Greenland, Atmos. Chem. Phys., 12, 4259–4277, doi:10.5194/acp-12-4259-2012, 2012.

Courville, Z. R., Albert, M. R., Fahnestock, M. A., Cathles, L. M., and Shuman, C. A.: Impacts of an accumulation hiatus on the physical properties of firn at a low-accumulation polar site, J. Geophys. Res.-Earth, 112, F02030, doi:10.1029/2005JF000429, 2007.

Courville, Z., Hörhold, M., Hopkins, M., and Albert, M.: Lattice-Boltzmann modeling of the air permeability of polar firn, J. Geophys. Res.-Earth, 115, F04032, doi:10.1029/2009JF001549, 2010.

Fabre, A., Barnola, J. M., Arnaud, L., and Chappellaz, J.: Determination of gas diffusivity in polar firn: Comparison between

experimental measurements and inverse modeling, Geophys. Res. Lett., 27, 557–560, 2000.

Faïn, X., Ferrari, C. P., Dommergue, A., Albert, M. R., Battle, M., Severinghaus, J., Arnaud, L., Barnola, J.-M., Cairns, W., Barbante, C., and Boutron, C.: Polar firn air reveals large-scale impact of anthropogenic mercury emissions during the 1970s, P. Natl. Acad. Sci. USA, 106, 16114–16119, 2009.

Freitag, J., Dobrindt, U., and Kipfstuhl, J.: A new method for predicting transport properties of polar firn with respect to gases on the pore-space scale, Ann. Glaciol., 35, 538–544, 2002.

Garboczi, E. J.: Permeability, diffusivity, and microstructural parameters: a critical review, Cement Concrete Res., 20, 591–601, 1990.

Goujon, C., Barnola, J.-M., and Ritz, C.: Modeling the densification of polar firn including heat diffusion: Application to close-off characteristics and gas isotopic fractionation for Antarctica and Greenland sites, J. Geophys. Res.-Atmos., 108, 4792, doi:10.1029/2002JD003319, 2003.

Gregory, S. A., Albert, M. R., and Baker, I.: Impact of physical properties and accumulation rate on pore close-off in layered firn, The Cryosphere, 8, 91–105, doi:10.5194/tc-8-91-2014, 2014.

Hörhold, M. W., Albert, M. R., and Freitag, J.: The Impact of Accumulation Rate on Anisotropy and Air Permeability of Polar Firn at a High Accumulation Site, J. Glaciol., 55, 625–630, 2009.

Katz, A. J. and Thompson, A. H.: Quantitative prediction of permeability in porous rock, Phys. Rev. B, 34, 8179–8181, 1986.

Lomonaco, R., Albert, M., and Baker, I.: Microstructural evolution of fine-grained layers through the firn column at Summit, Greenland, J. Glaciol., 57, 755–762, 2011.

Martinerie, P., Ya Lipenkov, V., Raynaud, D., Chappellaz, J., Barkov, N. I., and Lorius, C.: Air content paleo record in the Vostok ice core (Antarctica): A mixed record of climatic and glaciological parameters, J. Geophys. Res.-Atmos., 99, 10565–10576, 1994.

Matsunaga, N., Hori, M., and Nagashima, A.: Diffusion coefficients of global warming gases into air and its component gases, High Temp.-High Press., 30, 77–84, 1998.

Matsunaga, N., Hori, M., and Nagashima, A.: Measurements of the mutual diffusion coefficients of gases by the Taylor method (7th Report, measurements on the SF6-air, SF6-N2, SF6-O2, CFC12-N2, CFC12-O2, HCFC22-N2 and HCFC22-O2 systems), Trans. Jpn. Soc. Mech. Eng. B, 68, 550–555, 2002.

McGrath, D., Colgan, W., Bayou, N., Muto, A., and Steffen, K.: Recent warming at Summit, Greenand: Global context and implications, Geophys. Res. Lett., 40, 2091–2096, 2013.

Neftel, A., Oeschger, H., Schwander, J., Stauffer, B., and Zumbrunn, R.: Ice core sample measurements give atmospheric CO_2 content during the past 40,000 yr, Nature, 295, 220–223, 1982.

Nghiem, S. V., Hall, D. K., Mote, T. L., Tedesco, M., Albert, M. R., Keegan, K., Shuman, C. A., DiGirolamo, N. E., and Neumann, G.: The extreme melt across the Greenland ice sheet in 2012, Geophys. Res. Lett., 39, L20502, doi:10.1029/2012GL053611, 2012.

Raynaud, D., Jouzel, J., Barnola, J. M., Chappellaz, J., Delmas, R. J., and Lorius, C.: The ice record of greenhouse gases. Science, 259, 926–934, 1993.

Rick, U. K. and Albert, M. R.: Microstructure and permeability in the near-surface firn near a potential US deep-drilling site in West Antarctica, Ann. Glaciol., 39, 62–66, 2004.

Schwander, J.: The transformation of snow to ice and the occlusion of gases, in: The Environmental Record in Glaciers and Ice Sheets, edited by: Oeschger, H., Langway Jr., C. C., John Wiley & Sons, New York, 53–67, 1989.

Schwander, J., Stauffer, B., and Sigg, A.: Air mixing in firn and the age of the air at pore close-off, Ann. Glaciol., 10, 141–145, 1988.

Schwander, J., Barnola, J. M., Andrié, C., Leuenberger, M., Ludin, A., Raynaud, D., and Stauffer, B.: The age of the air in the firn and the ice at Summit, Greenland, J. Geophys. Res., 98, 2831–2838, 1993.

Schwartz, L. M., Martys, N., Bentz, D. P., Garboczi, E. J., and Torquato, S.: Cross property relations and permeability estimation in model porous media, Phys. Rev. E, 48, 4584–4591, 1993.

Spahni, R., Schwander, J., Flückiger, J., Stauffer, B., Chappellaz, J., and Raynaud, D.: The attenuation of fast atmospheric CH_4 variations recorded in polar ice cores, Geophys. Res. Lett., 30, 1571, doi:10.1029/2003GL017093, 2003.

Trudinger, C. M., Enting, I. G., Rayner, P. J., Etheridge, D. M., Buizert, C., Rubino, M., Krummel, P. B., and Blunier, T.: How well do different tracers constrain the firn diffusivity profile?, Atmos. Chem. Phys., 13, 1485–1510, doi:10.5194/acp-13-1485-2013, 2013.

Witrant, E., Martinerie, P., Hogan, C., Laube, J. C., Kawamura, K., Capron, E., Montzka, S. A., Dlugokencky, E. J., Etheridge, D., Blunier, T., and Sturges, W. T.: A new multi-gas constrained model of trace gas non-homogeneous transport in firn: evaluation and behaviour at eleven polar sites, Atmos. Chem. Phys., 12, 11465–11483, doi:10.5194/acp-12-11465-2012, 2012.